

# A Gravitational Aharonov-Bohm Effect, and its Connection to Parametric Oscillators and Gravitational Radiation

Raymond Y. Chiao<sup>1</sup>, Robert Haun<sup>2</sup>, Nader Inan<sup>2</sup>, Bong-Soo Kang<sup>2</sup>,  
Luis A. Martinez<sup>2</sup>, Stephen J. Minter<sup>3</sup>, Gerardo Muñoz<sup>4</sup>, and Douglas Singleton<sup>4,5</sup>

<sup>1</sup>University of California, Merced, Schools of Natural Sciences and Engineering, P.O. Box 2039, Merced, CA 95344, USA  
Corresponding author, email: rchiao@ucmerced.edu

<sup>2</sup>University of California, Merced, School of Natural Sciences, P.O. Box 2039, Merced, CA 95344, USA

<sup>3</sup>Vienna Center for Quantum Science and Technology, Faculty of Physics, University of Vienna, Boltzmannngasse 5, A-1090 Vienna, Austria

<sup>4</sup>California State University, Fresno, CA 93740, USA <sup>5</sup>Department of Physics, Institut Teknologi Bandung, Indonesia

PACS: 03.65.Ta, 04.30.-w, 04.80.Cc, 05.45.Xt, 42.65.Yj

## Abstract

A thought experiment is proposed to demonstrate the existence of a gravitational, vector Aharonov-Bohm effect. We begin the analysis starting from four Maxwell-like equations for weak gravitational fields interacting with slowly moving matter. A connection is made between the gravitational, vector Aharonov-Bohm effect and the principle of local gauge invariance for nonrelativistic quantum matter interacting with weak gravitational fields. The compensating vector fields that are necessitated by this local gauge principle are shown to be incorporated by the DeWitt minimal coupling rule. The nonrelativistic Hamiltonian for weak, time-independent fields interacting with quantum matter is then extended to time-dependent fields, and applied to problem of the interaction of radiation with macroscopically coherent quantum systems, including the problem of gravitational radiation interacting with superconductors. But first we examine the interaction of EM radiation with superconductors in a parametric oscillator consisting of a superconducting wire placed at the center of a high  $Q$  superconducting cavity driven by pump microwaves. Some room-temperature data will be presented demonstrating the splitting of a single microwave cavity resonance into a spectral doublet due to the insertion of a central wire. This would represent an *unseparated* kind of parametric oscillator, in which the signal and idler waves would occupy the same volume of space. We then propose a *separated* parametric oscillator experiment, in which the signal and idler waves are generated in two disjoint regions of space, which are separated from each other by means of an impermeable superconducting membrane. We find that the threshold for parametric oscillation for EM microwave generation is much lower for the separated configuration than the unseparated one, which then leads to an observable dynamical Casimir effect. We speculate that a separated parametric oscillator for generating coherent GR microwaves could also be built.

## 1 Introduction

In this paper we discuss three apparently distinct phenomena: The gravitational Aharonov-Bohm effect, the dynamical Casimir effect arising from parametric oscillations, and gravitational waves. The first of these phenomena is simply the gravitational version of the electromagnetic Aharonov-Bohm effect. There has been recent interest in the gravitational version of the *scalar* Aharonov-Bohm effect [1]. Here we will discuss the gravitational version of the *vector* Aharonov-Bohm effect. In the second phenomenon, i.e., the dynamical Casimir effect, we propose a possible experiment in which photons could be “pumped out of the vacuum” via a vibrating superconducting (SC) “membrane” considered as a parametric oscillator. Finally, we discuss gravitational waves. We speculate that a gravitational version of “pumping gravitons out of the vacuum” via parametric amplification, and above threshold, parametric oscillation, might be possible. The analog of a laser for gravitational waves could thus be constructed.

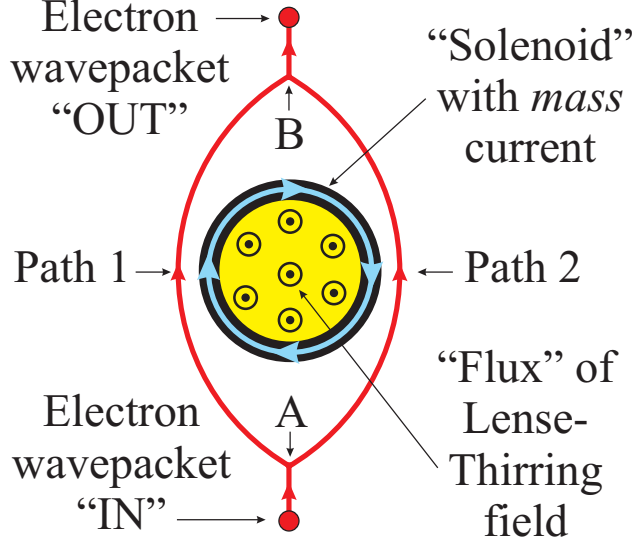


Figure 1: (Color online) Sketch of a gravitational Aharonov-Bohm effect. A “solenoid” with circulating mass currents (in blue), produces “flux” (black dots) of a certain “gravito-magnetic” field (the Lense-Thirring field) in its interior (in yellow). In its exterior (in white), this field is zero. Nevertheless, an electron wave packet (in red), which is split at point A to go around the “solenoid” via paths 1 and 2, and then recombined at point B, will exhibit an Aharonov-Bohm fringe shift.

The concept that links these three phenomena together is the use of the DeWitt minimal coupling rule, whereby particles are coupled to both the electromagnetic and the gravitational vector potential.

## 2 Gravitational Aharonov-Bohm effect

A gravitational analog of the vector Aharonov-Bohm effect is depicted in Figure 1 [1][2][3]. Aharonov-Bohm (AB) interference can occur when an incoming single-electron wavepacket is split at point A by means of a beam splitter into two partial waves traveling along paths 1 and 2, respectively, that go around the outside of a “solenoid” which contains circulating *mass* currents (indicated by the blue arrows).

For instance, such mass currents in a cylindrical superconducting (SC) mass shell (indicated in black in Figure 1), could be produced by rotating the shell at a constant angular frequency around its cylindrical axis. The two partial waves could then be recombined into an outgoing single-electron wavepacket at point B by means of another beam splitter. Just like in the purely electromagnetic AB effect, the “flux” of a certain gravito-magnetic field (i.e., the Lense-Thirring field) would be confined entirely to the interior region (indicated in yellow in Figure 1) of the “solenoid,” and would vanish at all points in its exterior (indicated in white). There results a quantum mechanical AB fringe shift due to the “flux” that is observable at point B, which cannot be explained classically.

To understand the thought experiment pictured in Figure 1, we begin from Einstein’s field equations, which, in the limit of weak gravitational fields near slowly moving matter (i.e., in the vicinity of nonrelativistic masses), become the following set of four Maxwell-like equations [4]:

$$\nabla \cdot \mathbf{E}_g = -\frac{\rho_g}{\epsilon_g} \quad (1)$$

$$\nabla \times \mathbf{E}_g = -\frac{\partial \mathbf{B}_g}{\partial t} \quad (2)$$

$$\nabla \cdot \mathbf{B}_g = 0 \quad (3)$$

$$\nabla \times \mathbf{B}_g = 4\mu_g \left( -\mathbf{j}_g + \epsilon_g \frac{\partial \mathbf{E}_g}{\partial t} \right) \quad (4)$$

where the gravitational analog  $\epsilon_g$  of the electric permittivity  $\epsilon_0$  of free space is [5]

$$\epsilon_g = \frac{1}{4\pi G} = 1.19 \times 10^9 \text{ SI units} \quad (5)$$

and where the gravitational analog  $\mu_g$  of the magnetic permeability  $\mu_0$  of free space is [6]

$$\mu_g = \frac{4\pi G}{c^2} = 9.31 \times 10^{-27} \text{ SI units} \quad (6)$$

Here  $G = 6.67 \times 10^{-11}$  SI units is Newton's constant, and  $c = 3.00 \times 10^8$  m s<sup>-1</sup> in SI units is the vacuum speed of light.

In the four Maxwell-like equations, (1) – (4), the electric-like field  $\mathbf{E}_g$  is the *gravito-electric* field, (i.e., the local acceleration  $\mathbf{g}$  of a freely falling test particle), which could be produced by the mass density  $\rho_g$  of nearby matter, via (1). Likewise, the magnetic-like field  $\mathbf{B}_g$  is the *gravito-magnetic* field, which could be produced by the mass current density  $\mathbf{j}_g$  of nearby nonrelativistically moving matter, and also by the gravitational analog of the Maxwell displacement current density  $\epsilon_g \partial \mathbf{E}_g / \partial t$ , via (4). In the case of nearby *stationary* nonrelativistic mass currents,  $\mathbf{B}_g$  can be identified with the Lense-Thirring field [7] that is generated by these currents.

A nonrelativistic test particle with a mass  $m$  moves in the presence of the weak fields  $\mathbf{E}_g$  and  $\mathbf{B}_g$  in accordance with the Lorentz-like force law [4]

$$\mathbf{F} = m \frac{d\mathbf{v}}{dt} = m(\mathbf{E}_g + \mathbf{v} \times \mathbf{B}_g) \quad (7)$$

where  $m$  is the mass of the test particle and  $\mathbf{v}$  is its velocity (with  $v \ll c$ ).

To understand the experiment pictured in Figure 1, we only need the *stationary* version of (4), i.e., the gravitational analog of Ampere's law

$$\nabla \times \mathbf{B}_g = -4\mu_g \mathbf{j}_g \quad (8)$$

where  $\mathbf{j}_g$  and  $\mathbf{B}_g$  do not depend on time. This implies the following gravitational analog of Ampere's circuital law:

$$\oint_C \mathbf{B}_g \cdot d\mathbf{l} = -4\mu_g (I_g)_{\text{enc}} \quad (9)$$

where  $d\mathbf{l}$  is a line element of an arbitrary closed curve  $C$ , and  $(I_g)_{\text{enc}}$  is the mass current which is enclosed by  $C$ . Applying this Ampere's circuital law to the “solenoid” of Figure 1, which could be a uniformly rotating SC cylindrical mass shell, and using an appropriately chosen closed curve  $C$ , one concludes that the  $\mathbf{B}_g$  field in the interior to the “solenoid” is a uniform field pointing along the cylindrical axis, and that it has a constant magnitude

$$B_g = 4\mu_g I'_g \quad (10)$$

where  $I'_g$  is the mass current per unit length of the “solenoid” flowing around the circumference of the rotating cylindrical mass shell. Furthermore, by another appropriate choice of the closed curve  $C$ , one concludes that everywhere outside the “solenoid,” it is the case that

$$B_g = 0 \quad (11)$$

i.e., that the Lense-Thirring field vanishes everywhere exterior to the “solenoid.” This is analogous to the fact that the magnetic field vanishes at all points outside of an electromagnetic solenoid. Hence it follows from the Lorentz-like force law (7) that although the electron in Figure 1 experiences a *radial* classical gravitational force due to the mass of the “solenoid,” it could never have experienced any *azimuthal* classical gravitational force on its way from point A to point B via either path 1 or path 2 that could have caused the AB phase shift.

Put differently, if one thinks of the “solenoid” as a rotating SC cylindrical mass shell, the experiment has two independent parameters, namely, the linear mass density, and the angular velocity of the shell. That means one could shift the interference fringes by changing the angular velocity. Since the gravito-electric field from the mass of the shell does not depend on the angular velocity, a fringe shift will happen despite the fact that the classical force has not changed. Hence the AB fringe shift in the gravitational case could not have had a classical origin.

Now from the Maxwell-like equation (3), and from the vector identity

$$\nabla \cdot (\nabla \times \mathbf{h}) = 0 \quad (12)$$

it follows that it is always possible to express the magnetic-like field  $\mathbf{B}_g$  as

$$\mathbf{B}_g = \nabla \times \mathbf{h} \quad (13)$$

for some vector field  $\mathbf{h}$ . The relationship (13) is formally identical to the relationship in electromagnetism between the magnetic field  $\mathbf{B}$  and the electromagnetic vector potential  $\mathbf{A}$

$$\mathbf{B} = \nabla \times \mathbf{A} \quad (14)$$

which follows from the Maxwell equation  $\nabla \cdot \mathbf{B} = 0$ . Therefore we shall call  $\mathbf{h}$  the “gravitational vector potential.”

In the gravitational case, just as in the electromagnetic case, the gravitational vector potential  $\mathbf{h}$  possesses the gauge freedom

$$\mathbf{h} \rightarrow \mathbf{h} + \nabla \mu \quad (15)$$

where  $\mu$  can be any arbitrary scalar function of position. This follows from the vector identity  $\nabla \times \nabla \mu = 0$ , and is formally identical to the case of electromagnetism, in which the vector potential  $\mathbf{A}$  possesses the gauge freedom

$$\mathbf{A} \rightarrow \mathbf{A} + \nabla \lambda \quad (16)$$

where  $\lambda$  can be any arbitrary scalar function of position. Again, this follows from the vector identity  $\nabla \times \nabla \lambda = 0$ .

Now the principle of *local* gauge invariance in nonrelativistic quantum mechanics states that the phase of the time-independent wavefunction  $\Psi(\mathbf{r})$  of any quantum system must always be able to be *locally* transformed without affecting the physics of the system. In other words, the transformation [8]

$$\Psi(\mathbf{r}) \rightarrow \Psi(\mathbf{r}) \exp(i\phi(\mathbf{r})) \quad (17)$$

where the phase  $\phi(\mathbf{r})$  can be any *arbitrary* real scalar function of position  $\mathbf{r}$ , can neither change the properties of the quantum system, nor the physical laws governing the system and its interactions with its environment. In particular, this *local* transformation of the phase of the wavefunction cannot change the probability distribution of the system, since

$$|\Psi(\mathbf{r})|^2 \rightarrow |\Psi(\mathbf{r}) \exp(i\phi(\mathbf{r}))|^2 = |\Psi(\mathbf{r})|^2 \quad (18)$$

and therefore the Born probability interpretation of the wavefunction is unaffected by this transformation.

However, *gradients* of  $\Psi(\mathbf{r})$  will be changed by the introduction of an *arbitrary* scalar function  $\phi(\mathbf{r})$ , and therefore will alter the momentum of the system. If so, one could *arbitrarily* alter the physical laws governing the system, including altering the conservation of momentum of a particle in the usual  $\exp(i\mathbf{p} \cdot \mathbf{r}/\hbar)$  plane wave state of an electron within a force-free region of space, where one knows that  $\mathbf{p}$  must be a constant. This obviously cannot be the case. Therefore the principle of local gauge invariance *necessitates* the existence of some compensating vector field (or fields), such as the  $\mathbf{A}$  and  $\mathbf{h}$  fields in the DeWitt minimal coupling rule [9]

$$\frac{\hbar}{i} \nabla \rightarrow \frac{\hbar}{i} \nabla - q\mathbf{A} - m\mathbf{h} \quad (19)$$

$$\mathbf{p} \rightarrow \mathbf{p} - q\mathbf{A} - m\mathbf{h} \quad (20)$$

where  $\mathbf{p}_{\text{op}} = \frac{\hbar}{i}\nabla$  is the momentum operator,  $q$  is the charge, and  $m$  is the mass of the nonrelativistic quantum system under consideration. Here  $\mathbf{A}$  and  $\mathbf{h}$  are, respectively, the vector potentials for electromagnetism and for weak gravitation, which are being viewed here as being the requisite “compensating vector fields,” whose existence is *necessitated* by the principle of local gauge invariance. Since the vector fields  $\mathbf{A}$  and  $\mathbf{h}$  have the gauge freedoms  $\mathbf{A}(\mathbf{r}) \rightarrow \mathbf{A}(\mathbf{r}) + \nabla\lambda(\mathbf{r})$  and  $\mathbf{h}(\mathbf{r}) \rightarrow \mathbf{h}(\mathbf{r}) + \nabla\mu(\mathbf{r})$ , these freedoms can then be used to compensate for the gauge freedom in the transformation  $\Psi(\mathbf{r}) \rightarrow \Psi(\mathbf{r}) \exp(i\phi(\mathbf{r}))$ , in just such a way that the quantum system can once again satisfy the principle of local gauge invariance.

Thus invoking the DeWitt minimal coupling rule (20), we demand that the nonrelativistic Hamiltonian of any quantum system in the presence of  $\mathbf{A}$  and  $\mathbf{h}$  fields must always have the following form [9]:

$$H = \frac{1}{2m} (\mathbf{p} - q\mathbf{A} - m\mathbf{h})^2 + V \quad (21)$$

where  $V$  is the potential energy of the system. Here, in the present context of the SC quantum systems that we are interested in, such as that of the SC “solenoid” pictured in Figure 1,  $q = 2e$  is the charge of a Cooper pair, and  $m = 2m_e$  is its mass.

Although one can always *arbitrarily* choose a gauge locally so that both vector fields  $\mathbf{A}$  and  $\mathbf{h}$  are set identically equal to zero at each point exterior to the solenoid, nevertheless the *fluxes* interior to the solenoid

$$\Phi = \oint_C \mathbf{A} \cdot d\mathbf{l} \quad (22)$$

$$\Phi_g = \oint_C \mathbf{h} \cdot d\mathbf{l} \quad (23)$$

where  $C$  is a closed curve enclosing the solenoid, cannot be arbitrarily set equal to zero, but must instead be gauge-invariant, nonzero, globally *measurable* quantities. Hence the fluxes  $\Phi$  and  $\Phi_g$  must be *physical* quantities.

The gravitational Aharonov-Bohm effect depicted in Figure 1 is closely related to the time holonomy which arises from the off-diagonal time-space components of the metric tensor  $g_{0i}$  [10]. It can be shown [11] that this time holonomy  $\Delta t$  can be expressed as follows:

$$\Delta t = -\frac{1}{c} \oint_C \frac{g_{0i}}{g_{00}} dx^i \quad (24)$$

where  $C$  is an arbitrary closed curve in space (such as the one enclosing the “solenoid” in Figure 1), and  $dx^i$  is a spatial line element of this closed curve. In light of the time holonomy given by (24), it is impossible in general relativity to define a global time coordinate for an entire physical system, such as the topologically nontrivial superconductor in Figure 1.

In the weak field, slow matter approximation, in which

$$g_{0i} \approx h_{0i} \quad (25)$$

where  $h_{0i}$  are the time-space components of the small-deviation metric  $h_{\mu\nu}$  from the Minkowski metric  $\eta_{\mu\nu}$ , and in which the time-time component of the metric can be approximated by

$$g_{00} \approx -1 \quad (26)$$

it follows that the time holonomy (24) becomes approximately

$$\Delta t \approx \frac{1}{c} \oint_C h_{0i} dx^i \quad (27)$$

For electron waves traveling around a closed curve  $C$  enclosing a “solenoid” such as that in Figure 1, the *time* holonomy (27) becomes the *phase* holonomy

$$\Delta\phi = \omega_{\text{Compton}} \Delta t \approx \frac{m_e c^2}{\hbar} \frac{1}{c} \oint_C h_{0i} dx^i \neq 0 \quad (28)$$

where  $\omega_{\text{Compton}} = m_e c^2 / \hbar$  is the Compton frequency of the electron [1]. The phase shift (28), which is nonvanishing for the “solenoid” configuration of Figure 1, is the gravitational AB phase shift. It is closely related to Berry’s phase [12], since both phases have a common origin in non-Euclidean geometry.

Since physically counting the number of fringes in a shift of an Aharonov-Bohm interference pattern, such that in Figure 1, must yield the same result for all observers, independent of their state of motion under a restricted set of (Galilean) coordinate transformations, it is sufficient for the purposes of this paper to say that the flux  $\Phi_G$  is a Galilean invariant, and therefore a measurable, *physical* quantity. Moreover, the closed-path integral of  $h_{0i} dx^i$  in (27) is an intrinsic time holonomy which cannot vanish due to an arbitrary gauge transformation.

However, if one were to *arbitrarily* make the global gauge choice

$$h_{0i} = 0 \text{ everywhere} \quad (29)$$

as is done, for example, in the transverse-traceless gauge, then it follows that the phase holonomy must vanish identically, i.e.,

$$\Delta\phi \approx \frac{mc^2}{\hbar} \frac{1}{c} \oint_C h_{0i} dx^i = 0 \text{ by setting } h_{0i} = 0 \text{ everywhere} \quad (30)$$

and the gravitational Aharonov-Bohm phase shift predicted for the electron interference pattern in Figure 1 would disappear.

However, just as in the case of the electromagnetic Aharonov-Bohm effect where

$$\Delta\phi = \frac{q}{\hbar} \oint_C A_i dx^i = 0 \text{ by setting } A_i = 0 \text{ everywhere} \quad (31)$$

the results (30) and (31) are both unphysical whenever the closed curve  $C$  encloses either a solenoid with a nonvanishing electromagnetic flux  $\Phi \neq 0$ , or a “solenoid” with a nonvanishing Lense-Thirring flux  $\Phi_g \neq 0$ , since both of these fluxes are gauge-invariant, measurable, physical quantities that cannot be arbitrarily set equal to zero. Hence the transverse-traceless gauge choice (29) is unphysical in situations that involve the gravitational Aharonov-Bohm effect depicted in Figure 1 where  $\Phi_g \neq 0$ , and also, by extension, in time-varying situations that involve  $\Phi_g(t) \neq 0$ , for example, in situations where gravitational radiation is interacting with superconducting systems.

The usual Aharonov-Bohm phase shift follows from DeWitt’s minimal coupling rule (20) when one sets  $\Phi_g = 0$ , for then the phase shift arising from (20) in the configuration pictured in Figure 1, reduces down to the usual expression

$$\Delta\phi = \frac{q}{\hbar} \oint_C \mathbf{A} \cdot d\mathbf{l} \neq 0 \quad (32)$$

and we recover the standard form for the AB phase shift. However, if  $\Phi_g \neq 0$ , then the total AB phase, upon integration over any closed curve  $C$  enclosing the “solenoid,” becomes

$$\Delta\phi_{\text{tot}} = \frac{q}{\hbar} \oint_C \mathbf{A} \cdot d\mathbf{l} + \frac{m}{\hbar} \oint_C \mathbf{h} \cdot d\mathbf{l} = \frac{q\Phi}{\hbar} + \frac{m\Phi_g}{\hbar} \quad (33)$$

The vector potential  $\mathbf{h}$  in (33) can arise either from a Lense-Thirring field, or from rotations of a quantum system, such as from a rotating SC ring. Since experiments with rotating SC systems are much easier to perform than experiments involving Lense-Thirring fields, we shall confine our attention for now to these much easier experiments.

One can check experimentally the expression given by (33) for a rotating SC ring, in which case the single-valuedness of the macroscopic wavefunction of the Cooper pairs demands that  $\Delta\phi_{\text{tot}} = 2\pi n$ , where  $n$  is an integer. It follows from this that a magnetic field must be generated by rotating a superconducting ring, i.e., that a “London moment” must accompany this rotation. Precision measurements of the London moment of a rotating SC ring thus provide a test for the correctness of the expression for

the total AB phase in (33). Cabrera and co-workers [13] performed these measurements to 100 parts per million. Thus the formula in (33) for the total AB phase has been experimentally verified. In this way, the expression in (20) for the DeWitt minimal coupling rule has been experimentally tested to high precision.

So far we have been considering only the case of stationary, time-independent, charge and mass currents, such as those in a SC magnet, or in a steadily rotating SC ring. These quantum currents can be the quantum mechanical sources of time-independent  $\mathbf{A}$  and  $\mathbf{h}$  fields that give rise to the AB effect.

### 3 The dynamical Casimir effect via parametric oscillations

In this section, we begin by discussing the case when the vector potentials  $\mathbf{A}$  and  $\mathbf{h}$  are time dependent, i.e.  $\mathbf{A}(\mathbf{r}, t)$  and  $\mathbf{h}(\mathbf{r}, t)$ . From this we will propose a version of the dynamical Casimir effect for the electromagnetic vector potential  $\mathbf{A}$ , in which photons are “pumped” out of the vacuum via parametric oscillations of a SC membrane.

It is natural to extend the time-independent Hamiltonian (21) to the following time-dependent one [14]:

$$H = \frac{1}{2m} (\mathbf{p} - q\mathbf{A}(\mathbf{r}, t) - m\mathbf{h}(\mathbf{r}, t))^2 + V \quad (34)$$

in which the fields  $\mathbf{A}(\mathbf{r}, t)$  and  $\mathbf{h}(\mathbf{r}, t)$  are to be first treated as classical fields, but the matter (e.g., the vibrating SC wire in Figure 2) is to be treated quantum mechanically, in the so-called “semi-classical approximation.”

Expanding the square in (34), one obtains the following interaction Hamiltonian terms:

$$H_{\mathbf{p}\cdot\mathbf{A}} = -\frac{q}{m}\mathbf{p}\cdot\mathbf{A}(\mathbf{r}, t) \quad (35)$$

which leads to the interaction of the quantum system with electromagnetic (EM) radiation, such as in the stimulated emission and absorption of EM waves by the quantum matter, and

$$H_{\mathbf{p}\cdot\mathbf{h}} = -\mathbf{p}\cdot\mathbf{h}(\mathbf{r}, t) \quad (36)$$

which leads to the interaction of the quantum system with gravitational (GR) radiation, such as in the stimulated emission and absorption of GR waves by the quantum matter, and

$$H_{\mathbf{A}\cdot\mathbf{h}} = +q\mathbf{A}(\mathbf{r}, t)\cdot\mathbf{h}(\mathbf{r}, t) \quad (37)$$

which leads to the interaction between EM and GR radiation fields mediated by the quantum system, such as in the transduction of EM waves into GR waves mediated by the quantum matter [15], and

$$H_{\mathbf{A}\cdot\mathbf{A}} = +\frac{q^2}{2m}\mathbf{A}(\mathbf{r}, t)\cdot\mathbf{A}(\mathbf{r}, t) \quad (38)$$

which leads to Landau-diamagnetism type of interactions of the quantum system with EM radiation, such as in the parametric amplification of EM waves by a strongly driven, i.e., “pumped,” quantum system (see, for example, Figures 2 and 4), and

$$H_{\mathbf{h}\cdot\mathbf{h}} = +\frac{m}{2}\mathbf{h}(\mathbf{r}, t)\cdot\mathbf{h}(\mathbf{r}, t) \quad (39)$$

which leads to *gravitational* Landau-diamagnetism type of interactions of the quantum system with GR radiation, such as in the parametric amplification of GR waves, again by a strongly driven, i.e., “pumped,” quantum system (again, see, for example, Figures 2 and 4).

All of the above interaction terms will be treated as small perturbations of the unperturbed Hamiltonian

$$H_0 = \frac{\mathbf{p}^2}{2m} + V \quad (40)$$

and can thus be treated using standard perturbation theory.

At a fully quantum mechanical level of description, both the matter and the radiation fields  $\mathbf{A}$  and  $\mathbf{h}$  would have to be quantized. The radiation fields could be quantized by invoking the commutation relations

$$[a, a^\dagger] = 1 \quad (41)$$

$$[b, b^\dagger] = 1 \quad (42)$$

where  $a$  and  $a^\dagger$  are, respectively, the annihilation and creation operators for a quantum of a single mode of the EM radiation field, and where  $b$  and  $b^\dagger$  are, respectively, the annihilation and creation operators for a quantum of a single mode of the GR radiation field.

For now, let us focus solely on the interactions of quantized EM radiation with matter. The second quantized form for the EM vector potential operator  $A_{\text{Op}}(\mathbf{r})$ , when summed over all the modes of a cavity enumerated by the index  $\kappa$ , is [16]

$$A_{\text{Op}}(\mathbf{r}) = \sum_{\kappa} \sqrt{\frac{\hbar}{2\epsilon_0\omega_{\kappa}}} (a_{\kappa} + a_{\kappa}^{\dagger}) \mathcal{E}_{\kappa}(\mathbf{r}) \quad (43)$$

where  $\omega_{\kappa}$  is the frequency of mode  $\kappa$ , and  $\mathcal{E}_{\kappa}(\mathbf{r})$  is one Cartesian component of the classical electric field distribution associated with this mode. Therefore, when there is a single dominant mode in the problem, the vector potential operator simplifies to the expression

$$A_{\text{Op}}(\mathbf{r}) \propto (a + a^\dagger) \quad (44)$$

where the mode index  $\kappa$  and the proportionality constant have been suppressed.

The expansion of the square in the interaction Hamiltonian  $H_{\mathbf{A},\mathbf{A}} \propto (a + a^\dagger)^2$  in (38) will therefore contain the term [17]

$$K_{\text{Op}} \propto a^\dagger a^\dagger + \text{hermitian adjoint} \quad (45)$$

The  $a^\dagger a^\dagger$  term of the operator  $K_{\text{Op}}$  corresponds to the process of photon *pair creation* in the parametric amplification arising from the pumping action of some strong “pump” wave upon a quantum system. It can be shown that (45) has the form of an infinitesimal generator of a squeezed state of light [17].

Instead of enumerating all the possible resulting second quantized forms of the above interaction Hamiltonian terms, let us just focus on one such term, namely,  $H_{\mathbf{A},\mathbf{A}}$  in (38), which is associated with parametric amplification, such as that in the setup depicted in Figure 2. This Figure represents an “opto-mechanical” parametric amplifier, which becomes, above threshold, a parametric oscillator, whose active element is the central vibrating SC wire (indicated in red), placed across the middle of an extremely high- $Q$  SC microwave cavity. Here, instead of using optical cavities, as is usual in ongoing opto-mechanical experiments [18], we shall be using SC microwave cavities. The reason for this is that the quality factor for SC microwave cavities has already been demonstrated by Haroche and co-workers [19] to be on the order of

$$Q \sim 10^{10} \quad (46)$$

which can be much higher than that of typical optical cavities.

The motion of the SC wire in the middle of the microwave cavity will modulate the “pump” microwaves coming through the “IN” port so as to produce radiation at new sideband frequencies via the Doppler effect. The “seed” radiation initially in one of these sidebands, namely, the first “Stokes” sideband, can then become the exponentially amplified. Macroscopic, easily detectable radiation in the form of a strong Stokes wave emitted by the parametric amplifier can then leave the cavity through the “OUT” port. This kind of strong Stokes emission would be similar to the Stokes emission observed in the stimulated Raman effect in nonlinear optics [20].

However, here we shall first analyze classically the parametric amplification process in Figure 2, in order to answer the following questions: What is the threshold for parametric oscillation in Figure 2? Is this experiment feasible to perform? The key concept that we shall use in this classical analysis is that of the *work done* by the moving wire, viewed as if the wire were a moving “piston” acting on some “seed”



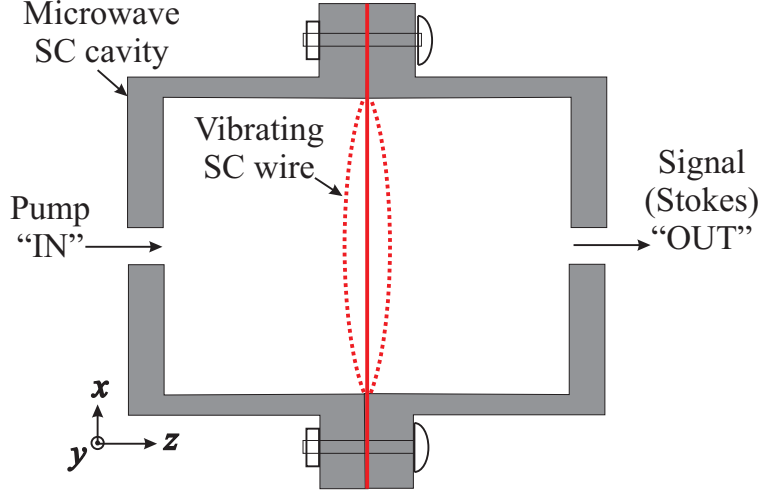


Figure 2: (Color online) A parametric amplifier or oscillator, whose active element is the vibrating SC wire (in red) placed in the middle of a microwave SC cavity (in grey). The moving wire can be viewed as if it were an oscillating “semipermeable membrane,” which does work upon some “seed” radiation initially present in the cavity, thus amplifying this radiation in a reciprocating, piston-like action. Photons incident upon this moving “membrane” experience a Doppler shift that changes their energy. Thus when pump microwaves enter through the left hole, an amplified signal (Stokes) wave will exit through the right hole.

radiation initially present in the cavity. This “piston-like” action of the moving wire can also be viewed as if the wire were a partially reflecting “moving mirror,” and will lead to the *exponential* amplification of the “seed” radiation at the Stokes frequency above the threshold of parametric oscillation.

The reason for using a vibrating wire instead of a vibrating membrane is that the wire is one dimensional, whereas the membrane is two dimensional. The mass of a thin wire can be made much smaller than the mass of a thin membrane, and therefore a wire can be driven more easily into motion.

However, here we shall model the vibrating wire in Figure 2 as if the wire were a vibrating “semi-permeable membrane,” for which the pressure acting on the membrane can be converted into an easily calculable force. The justification for this “membrane” model is that the scattering cross section of a thin conducting wire, when placed symmetrically across the mouth of a waveguide, can be comparable in size to the cross-sectional area of the waveguide, because the wire tends to “short out” the electric field of the TE mode of a waveguide. Thus the reflection coefficient of the wire placed across the middle of a cavity (as in Figure 2), can be made quite high. There results a splitting of a microwave cavity mode into a spectral doublet as illustrated in Figure 3 [21][22], due to the presence of the central wire. The splitting frequency of the doublet can typically be on the order of 1 GHz for a microwave mode frequency of around 10 GHz.

We have observed the splitting of a microwave cavity resonance into a spectral doublet. An RF cylindrical copper cavity of length  $L = 1.284$ ” and diameter  $D = 1.02$ ” with two parallel conducting end plates was constructed to support a TE<sub>112</sub> mode at 11.42 GHz [23]. (The mode indices  $l, m, n$  are chosen to correspond to the number of half wavelengths along their respective axes; angular, radial, and axial respectively.) The input coupler, a short straight wire placed perpendicular to the axial direction, was placed on the cylinder at approximately a quarter wavelength from one end plate. The output coupler is a small loop placed at the other end plate of the cavity.

An off-diagonal scattering matrix element S<sub>21</sub> transmission measurement, performed with a HP 8720C network analyzer, shows the resonance of the TE<sub>112</sub> mode at approximately 11.50 GHz; see figure 4(a). A splitting is observed by placing a 22AWG copper wire at the midpoint of the cavity, perpendicular to the axial direction and parallel to the input coupler. The splitting is approximately 400 MHz; see figure 4(b).

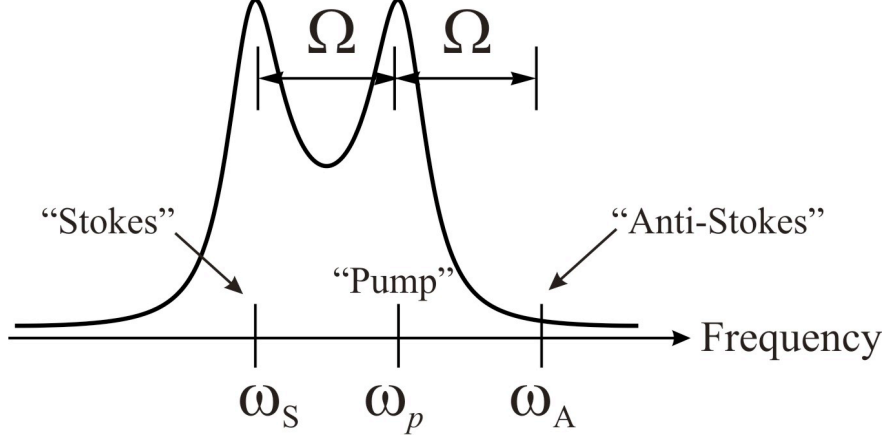


Figure 3: The excitation spectrum of a microwave cavity with a wire placed at its center (see Figure 2). The spectrum consists of a doublet of resonances at the “signal” mode at the “Stokes” frequency  $\omega_S$  and the “pump” mode at the “pump” frequency  $\omega_p$ . The difference between “pump” and “Stokes” frequencies is resonant with the frequency  $\Omega$  of the vibrating wire (i.e.,  $\omega_p - \omega_S = \Omega$ ). The “anti-Stokes” frequency  $\omega_A$  is off resonance with respect to the doublet, and hence is suppressed. (Cf. the stimulated Raman effect in [20]).

In Figure 3, the pump frequency  $\omega_p$  of the parametric amplifier is assumed to be tuned to coincide with the upper member of the spectral doublet, and the signal frequency  $\omega_S$  is assumed to be tuned to coincide with the lower member of this doublet, which we shall call the “Stokes frequency,” in analogy with the stimulated Raman effect [20]. The idler frequency  $\omega_i$ , i.e., the frequency of the mechanical motion of the central wire in Figure 2, is the beat frequency  $\Omega = \omega_p - \omega_S$  between the pump and signal frequencies. Note that the parasitic, Doppler upshifted “anti-Stokes frequency”  $\omega_A$  is automatically suppressed by this spectral doublet.

To calculate the force acting on the central membrane (as a model of the force acting on the central wire) in the middle of the microwave cavity of Figure 2, we begin from the Maxwell stress tensor [24][25]

$$T_{ij} = \epsilon_0 \left( E_i E_j - \frac{1}{2} \delta_{ij} E^2 \right) + \frac{1}{\mu_0} \left( B_i B_j - \frac{1}{2} \delta_{ij} B^2 \right) \quad (47)$$

Now starting from the electromagnetic force exerted on charges and currents given by the Lorentz force law

$$\mathbf{F} = q(\mathbf{E} + \mathbf{v} \times \mathbf{B}) \quad (48)$$

it can be shown that there results the following relationship between the force  $\mathbf{F}$  and the total Maxwell stress tensor  $T_{ij}$  and the Poynting vector  $\mathbf{S}$  [24][25]:

$$(\mathbf{F})_i = \oint_{S(V)} T_{ij} \cdot (d\mathbf{a})^j - \epsilon_0 \mu_0 \frac{d}{dt} \int_V (\mathbf{S})_i dV \quad (\text{where } i = 1, 2, 3) \quad (49)$$

where  $T_{ij}$  is the stress tensor evaluated at  $d\mathbf{a}$ , an infinitesimal area element of an arbitrary surface  $S(V)$  which encloses the volume  $V$ ,  $dV$  is an infinitesimal volume element of the matter inside the volume  $V$  enclosed by the surface  $S(V)$ , and  $\mathbf{S} = \mathbf{E} \times \mathbf{H}$  is the Poynting vector evaluated at  $dV$  inside  $V$ .

Now the tangential electric field must vanish at the boundary of any conductor. Hence, for all transverse electric modes of the microwave cavity pictured in Figure 2, if one chooses the surface  $S(V)$  to be that of a small pillbox straddling a patch of the surface of an equivalent SC membrane, the contribution to the force (49) from the Poynting vector term evaluated at the pillbox enclosing the patch of the surface, must vanish. In the case of transverse magnetic modes of the cavity, the Poynting vector  $\mathbf{S} = \mathbf{E} \times \mathbf{H}$  does

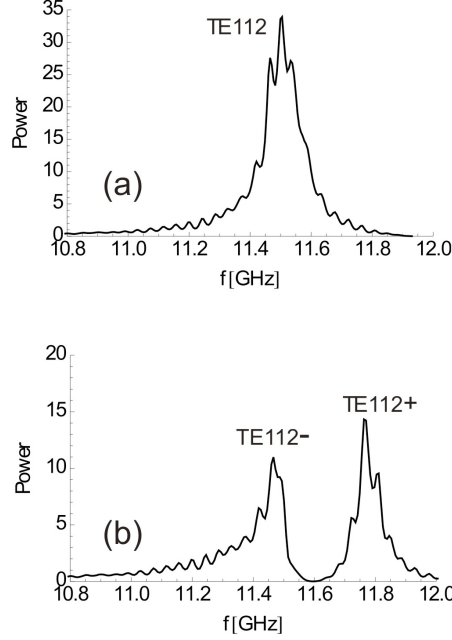


Figure 4: Splitting of the TE112 mode in cavity with a bisecting copper wire at its midpoint perpendicular to the axial direction and parallel to the input coupler. The splitting is on the order of 400 MHz. S21 transmission measurements (a) of a copper cavity with TE112 resonant frequency at 11.5 GHz and (b) splitting due to the placement of copper wire placed at the center. The vertical axes use the same arbitrary power reference in the conversion from logarithmic to linear scale.

not vanish at the surface, since there will be a longitudinal component of the electric field at the surface along with a tangential component of the magnetic field. Hence there will arise a *tangential* component of  $\mathbf{S}$  at the surface of the SC membrane, but this  $\mathbf{S}$  cannot contribute to any *normal* force acting on the conducting surface.

Therefore the only contribution to the normal force acting on the equivalent SC membrane arises solely from the Maxwell stress tensor term of (49), which, for the case of transverse electric modes evaluated at the membrane, reduces down to

$$(T_{ij}) = \frac{1}{2\mu_0} \begin{pmatrix} -B_y^2 & 0 & 0 \\ 0 & +B_y^2 & 0 \\ 0 & 0 & -B_y^2 \end{pmatrix} \quad (50)$$

because the magnetic field of the transverse electric mode (e.g., the TE112 mode), whose electric field is pointing in the  $x$  direction (in the Cartesian coordinate system of Figure 2), will be pointing in the  $y$  direction at the surface of the equivalent membrane [26].

If one therefore replaces the SC wire by an equivalent SC membrane, then the diagonal terms of (50) can be interpreted as a “field pressure” acting on the membrane with a maximum amplitude of

$$P_{\max} = \frac{1}{2\mu_0} (B^2)_{\max} = (u_B)_{\max} \quad (51)$$

where  $(B^2)_{\max}$  is the maximum of the square of the magnetic field, and  $(u_B)_{\max}$  is the maximum magnetic energy density, evaluated at the surface of the membrane.

Because the stress tensor depends *quadratically* on the field, there results a pressure being exerted on the membrane at a beat note frequency due to the beating between the fields at pump frequency  $\omega_p$  and the fields at the Stokes frequency  $\omega_S$  in the spectral doublet of Figure 4. This beat note can drive

the membrane (or the wire) at the beat frequency  $\Omega = \omega_p - \omega_S$ , i.e., at the splitting of the upper and lower members of the doublet. The force in the  $z$  direction acting on the membrane (or wire) at the beat frequency  $\Omega$  will therefore have the form

$$\begin{aligned} F_\Omega &= \frac{1}{\mu_0} \mathcal{B}_p \mathcal{B}_S^* \exp(-i(\omega_p - \omega_S)t) \cdot \mathcal{A}_{\text{eff}} + \text{c.c.} \\ &\propto \exp(-i\Omega t) + \text{c.c.} \end{aligned} \quad (52)$$

where  $\mathcal{A}_{\text{eff}}$  is an effective area of the membrane (or, equivalently, the effective scattering cross-section of the wire), and where

$$B_p = \mathcal{B}_p \exp(-i\omega_p t) + \text{c.c.} \quad (53)$$

is the pump waveform, with  $\mathcal{B}_p$  being the complex amplitude for the pump magnetic field waveform, and where

$$B_S = \mathcal{B}_S \exp(-i\omega_S t) + \text{c.c.} \quad (54)$$

is the Stokes waveform of some small amount of “seed” radiation already present inside the cavity, with  $\mathcal{B}_S$  being the complex amplitude for the Stokes magnetic field waveform. (Note that such “seed” radiation could in principle be vacuum fluctuations of the EM field inside the cavity.) In the expression (52) for the force  $F_\Omega$  at the beat frequency  $\Omega$ , we have assumed that the pump wave (53) is always much stronger than the “seed” Stokes wave (54), i.e.,  $|\mathcal{B}_p| \gg |\mathcal{B}_S|$ .

Since the driving force  $F_\Omega$  at the beat frequency  $\Omega$  can be made resonant with the acoustical resonance frequency of the membrane, we shall model the resulting motion of the membrane as that of a simple harmonic oscillator with a resonance frequency of  $\Omega$ . Using Newton’s equation of motion for a damped simple harmonic oscillator moving in the  $z$  direction, viz.,

$$m(\ddot{z} + \gamma\dot{z} + \Omega^2 z) = F_\Omega \quad (55)$$

where  $m$  is the mass of the membrane, and  $\gamma$  is its damping coefficient, and using an Ansatz of the form

$$z = z_{\text{max}} \exp(-i\Omega t) + \text{c.c.} \quad (56)$$

for the displacement of the membrane in the  $z$  direction, one finds that its maximum, on-resonance complex displacement amplitude is

$$z_{\text{max}} = i \frac{\mathcal{B}_p \mathcal{B}_S^*}{\mu_0 m \gamma \Omega} \mathcal{A}_{\text{eff}} \quad (57)$$

The velocity of the membrane in the  $z$  direction will then have the form

$$v = v_{\text{max}} \exp(-i\Omega t) + \text{c.c.} \quad (58)$$

where the complex velocity amplitude  $v_{\text{max}} = -i\Omega z_{\text{max}}$  becomes, on resonance,

$$v_{\text{max}} = \frac{\mathcal{B}_p \mathcal{B}_S^*}{\mu_0 m \gamma} \mathcal{A}_{\text{eff}} \quad (59)$$

There results a Doppler effect arising from the velocity of the membrane moving in the  $z$  direction in Figure 2, giving rise to upper and lower Doppler sidebands. However, only the lower Doppler sideband will be excited, since only the lower sideband will be resonant with lower member of the doublet in Figure 4.

The maximum, on-resonance time-averaged power  $\langle P \rangle$  being delivered from the pump wave into the simple-harmonic membrane motion at the beat frequency  $\Omega$ , and therefore into the lower Doppler sideband, i.e., into the Stokes wave (54), is

$$\langle P_{\text{max}} \rangle = \langle F_\Omega \cdot v \rangle_{\text{max}} = 2 |\mathcal{B}_p|^2 |\mathcal{B}_S|^2 \frac{1}{\mu_0^2 m \gamma} \mathcal{A}_{\text{eff}}^2 \quad (60)$$

Now invoking the conservation of energy, we find that, if we for the moment neglect all losses, the Stokes wave will be amplified by this power transfer, such that the power  $\langle P_{\max} \rangle$  being transferred into the Stokes wave must equal the rate of growth of the time-averaged Stokes energy inside the cavity

$$\langle U_S \rangle = \frac{1}{\mu_0} |\mathcal{B}_S|^2 V_{\text{eff}} = \frac{1}{\mu_0} |\mathcal{B}_S|^2 \mathcal{A}_{\text{eff}} \mathcal{L}_{\text{eff}} \quad (61)$$

where  $\mathcal{L}_{\text{eff}}$  is an effective length of the cavity (i.e.,  $V_{\text{eff}} = \mathcal{A}_{\text{eff}} \mathcal{L}_{\text{eff}}$  is an effective volume of the cavity). In other words, from energy conservation it follows that

$$\langle P_{\max} \rangle = \frac{d}{dt} \langle U_S \rangle \quad (62)$$

Substituting in from (60) and (61), one infers that

$$2 |\mathcal{B}_p|^2 |\mathcal{B}_S|^2 \frac{1}{\mu_0^2 m \gamma} \mathcal{A}_{\text{eff}}^2 = \frac{d}{dt} \left( \frac{1}{\mu_0} |\mathcal{B}_S|^2 \mathcal{A}_{\text{eff}} \mathcal{L}_{\text{eff}} \right) = \kappa_S \left( \frac{1}{\mu_0} |\mathcal{B}_S|^2 \mathcal{A}_{\text{eff}} \mathcal{L}_{\text{eff}} \right) \quad (63)$$

where  $\kappa_S$  is the exponential gain coefficient for parametric amplification of the Stokes wave. Thus we arrive at an exponential-growth ODE for the energy stored  $U_S$  in the cavity at the Stokes frequency

$$\frac{d}{dt} \langle U_S \rangle = \kappa_S \langle U_S \rangle \quad (64)$$

Solving for the gain coefficient  $\kappa_S$  from (63), we conclude that

$$\kappa_S = \frac{2 |\mathcal{B}_p|^2 \mathcal{A}_{\text{eff}}}{\mu_0 m \gamma \mathcal{L}_{\text{eff}}} \quad (65)$$

Thus the gain of the Stokes wave is directly proportional to the pump power stored in the cavity, just like in the stimulated Raman effect [20].

Like in a laser, the threshold for oscillation [27][28] occurs when

$$\text{Gain} = \text{Loss} \quad (66)$$

Above threshold, i.e., when the gain exceeds the loss, macroscopic amounts of coherent radiation can be produced inside the cavity by the *exponential* amplification of the “seed” radiation, i.e., of vacuum fluctuations. Thus even if one were to start off only with vacuum fluctuations as the “seed,” one can produce macroscopic amounts of coherent radiation by the stimulated emission of radiation, just like in a laser. In principle, this should also apply to GR radiation, as well as to EM radiation. Thus *generators* of microwave frequency GR radiation should *in principle* be possible to construct, as well as amplifiers and detectors for this kind of radiation. The only remaining question is whether such devices are feasible *in practice*.

The loss of the Stokes wave (i.e., the “signal”) from the cavity depicted in Figure 2 can result from emission of radiation through an outcoupling hole into the environment, or from remnant ohmic losses in the components of the cavity. We shall call the resulting quality factor of the cavity at the Stokes frequency under working conditions (i.e., including internal losses and the outcoupling into the environment) the “loaded  $Q$ ”, which is defined as follows:

$$Q_S = \omega_S \tau_S \quad (67)$$

where “S” stands for “Stokes wave” whose frequency is  $\omega_S$ , and whose stored energy inside the cavity decays away with a time scale  $\tau_S$  (the so-called “cavity ring-down time”) after the pump has been turned off.

Moreover, the loss coefficient  $\gamma$  in the motion of the simple harmonic oscillator leads a decay time  $\tau_\Omega = 1/\gamma$  for the energy stored in the oscillator. This leads to a mechanical oscillator quality factor  $Q_\Omega$ , which is defined as follows:

$$Q_\Omega = \Omega \tau_\Omega \quad (68)$$

It follows from the gain-equals-loss condition (66) that at threshold

$$(\kappa_S)_{\text{threshold}} = \frac{2|\mathcal{B}_p|_{\text{threshold}}^2 \mathcal{A}_{\text{eff}}}{\mu_0 m \gamma \mathcal{L}_{\text{eff}}} = \frac{2|\mathcal{B}_p|_{\text{threshold}}^2 Q_\Omega \mathcal{A}_{\text{eff}}}{\mu_0 m \Omega \mathcal{L}_{\text{eff}}} = \frac{1}{\tau_S} = \frac{\omega_S}{Q_S} \quad (69)$$

Since the time-averaged stored energy in the pump wave inside the cavity depicted in Figure 2 is

$$\langle U_p \rangle = \frac{1}{\mu_0} |\mathcal{B}_p|^2 \mathcal{A}_{\text{eff}} \mathcal{L}_{\text{eff}} \quad (70)$$

we conclude from (69) that the threshold pump power needed for parametric oscillation is

$$\langle U_p \rangle_{\text{threshold}} = \frac{1}{2} \frac{m \Omega \omega_S \mathcal{L}_{\text{eff}}^2}{Q_S Q_\Omega} \quad (71)$$

This result is to be compared with the threshold pump power needed for parametric oscillation for exciting an elastic mode of a mirror of a Fabry-Perot resonator obtained by Braginsky and co-workers [27]

$$\langle U_p \rangle_{\text{Braginsky}} = \frac{1}{2} \frac{m \omega_s^2 L^2}{Q_i Q_s} \quad (72)$$

where  $m$  is the mass of the mirror,  $\omega_s$  is the frequency of the elastic mode,  $L$  is the length of the Fabry-Perot resonator,  $Q_i$  is the quality factor of a down-shifted “idler” optical mode of the resonator, and  $Q_s$  is the quality factor of the elastic mode. By inspection of (71) and (72), we see that these thresholds are quite similar.

However, the electrodynamic  $Q$  factor of SC microwave cavities is typically on the order of  $10^{10}$  [19], whereas the typical mechanical  $Q$  factor for the best opto-mechanical oscillators, which are composed of non-SC materials in the ongoing opto-mechanical experiments, is at most on the order of  $10^5$  [18]. Therefore the question naturally arises whether it is possible to replace these low- $Q$ , non-SC mechanical oscillators, with high- $Q$  SC mechanical oscillators, in which their mechanical  $Q$  can approach the typical electrodynamic  $Q \sim 10^{10}$  of SC microwave cavities.

One possible answer to this question is the “triple SC microwave Fabry-Perot resonator” shown in Figure 4 [21], in which a *charged* SC membrane is extremely tightly coupled via its electrostatic charge to the longitudinal electric fields of a transverse magnetic mode of a high  $Q$  SC microwave cavity. The idea here is that when the charge on the SC membrane is sufficiently large, then the mechanical dynamics of the membrane will be “slaved” to follow closely the electromagnetic dynamics of the high- $Q$  microwave SC mode. Calculations [29] show that one only needs a charge of pico-Coulombs for this to happen. Note that as a result of the “slaved” dynamics, the SC membrane will be moving at microwave, and not at acoustical, frequencies. This means that the motion of the membrane will be essentially that of a “free” mass, which is being driven solely by Maxwell’s stress tensor. Therefore this microwave-frequency motion will be independent of the elastic and dissipative mechanical properties of the membrane.

Another important feature of the configuration shown in Figure 4 is that the signal and the idler waves are *spatially separated* into two disjoint, high  $Q$  SC cavities, which are separated from each other by a common, vibrating SC membrane. It turns out that this leads to two *separate*  $Q$  factors in its denominator of the threshold for parametric oscillation, which arises due to this separation. We shall therefore call the parametric oscillator configuration of Figure 4 a “separated parametric oscillator,” in contrast to that in Figure 2, which we shall call an “unseparated parametric oscillator.” The threshold for the separated parametric oscillator of Figure 4 will turn out to be at least a factor of  $10^5$  lower than that of the unseparated parametric oscillator of Figure 2.

We start the analysis of the separated parametric amplifier depicted in Figure 4 by examining the work done by the “pump” wave on the moving SC “membrane,” when it produces a displacement by an amount  $\Delta z$  of the membrane to the left along the axis of the “double” Fabry-Perot resonator on the right side of the membrane. The work done during this displacement is

$$\Delta W = \left( \frac{1}{2\mu_0} B^2 \right) \cdot \mathcal{A}_{\text{eff}} \Delta z \quad (73)$$

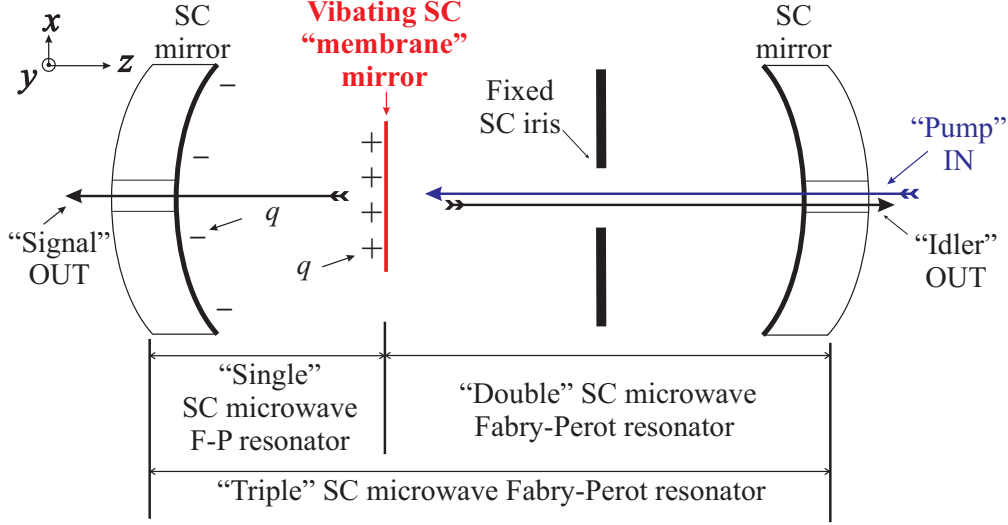


Figure 5: (Color online) A “triple” SC microwave Fabry-Perot cavity [21] consists of a “single” SC cavity separated by a vibrating SC “membrane” (in red) from a “double” SC cavity with a fixed SC iris (in black) at its center. This separating membrane is totally *impermeable* to all microwaves. The membrane is electrostatically charged on its left surface with a charge  $+q$ , and the left SC mirror is charged on its right surface with a charge  $-q$ . “Pump” microwaves (in blue) enter into the system through the right hole, and “signal” waves leave the system through the left hole, but “idler” waves leave the system through the right hole.

where  $\mathcal{A}_{\text{eff}}$  is the effective hemiconfocal spot size at the membrane,  $\Delta z$  is the displacement of this membrane, and

$$u_B = \frac{1}{2\mu_0} B^2 \quad (74)$$

is the energy density of the magnetic field evaluated at the right surface of the “membrane,” which is the pressure arising from the Maxwell stress tensor (50), i.e., a pressure being exerted upon the membrane that can cause a change of the volume inside the “double” Fabry-Perot resonator on the right side of the membrane

$$\Delta V = \mathcal{A}_{\text{eff}} \Delta z \quad (75)$$

where  $\mathcal{A}_{\text{eff}}$  is the effective area of the membrane, which is determined by the hemiconfocal spot size of the mode on the right side of the membrane. For simplicity, we shall assume here that the hemiconfocal spot size of the mode on the left side of the membrane also has the same  $\mathcal{A}_{\text{eff}}$ .

The instantaneous mechanical work  $\Delta W$  in (73) done by the “pump” upon the fields of the resonator can be rewritten in the form

$$\Delta W = P \Delta V \quad (76)$$

where the instantaneous pressure  $P$  on the “membrane” is

$$P = \frac{1}{2\mu_0} B^2 \quad (77)$$

which is equal to the instantaneous energy density  $u_B$  in (74) evaluated at the right surface of the membrane. It is clear from the expression for the work in (76) that  $\Delta W$  can be interpreted as if it were the work being done by a moving piston acting on a thermodynamic system, here, the radiation fields inside a cavity.

Now we shall presently see that if energy were to be continually supplied to the “double Fabry-Perot” resonator on the right side of the membrane by some continuous-wave, external microwave pump

waveform oscillating at a frequency  $\omega_p$  (i.e., the “pump” frequency) entering through the right hole of Figure 4, then the exponential amplification of some seed “signal” waveform at a frequency of  $\omega_s$  within the “single” Fabry-Perot on the left side of the membrane, simultaneously with the exponential amplification of some seed “idler” waveform at a frequency of  $\omega_i$  within the “double” Fabry-Perot on the right side of the membrane, can occur. This amplification effect can arise from the mutual reinforcement of the signal and idler waves at the expense of the pump wave, in which the pump wave beats with the idler wave via the Maxwell stress tensor to produce more of the signal wave, and the signal wave modulates the pump wave via the Doppler effect to produce more of the idler wave, etc. The mutual reinforcement of the two “seed” waves will lead to an instability above a certain threshold, i.e., to the parametric oscillation of both the signal and idler waves that produces macroscopic amounts of both kinds of waves, which then leave the system in opposite directions via the left hole and the right hole of Figure 4, respectively, just like in a laser.

For parametric amplification to occur, the frequency-matching condition

$$\omega_p = \omega_s + \omega_i \quad (78)$$

must be satisfied. The meaning of the relationship can be most easily seen by multiplying it by the Planck’s constant  $\hbar$  so that one obtains the relationship

$$\hbar\omega_p = \hbar\omega_s + \hbar\omega_i \quad (79)$$

In other words, in the parametric amplification process, one signal photon  $\hbar\omega_s$  is simultaneously created along with one idler photon  $\hbar\omega_i$  at the expense of one pump photon  $\hbar\omega_p$ , which is annihilated during this “photon pair-creation process.” In this process, an entangled pair of signal and idler photons, with the signal photon appearing on the left side, and the idler photon appearing on the right side of the membrane, respectively, will be produced in a correlated emission event inside the “triple” Fabry-Perot resonator depicted in Figure 4. This photon pair-creation process is described by the interaction Hamiltonian

$$H_{\text{int}} \propto a_p a_s^\dagger a_i^\dagger + \text{hermitian adjoint} \quad (80)$$

which is a generator of a *two-mode* squeezed state [16].

Let the microwave pump magnetic field just outside of the right surface of the membrane have the form

$$B_p = \mathcal{B}_p \exp(-i\omega_p t) + \text{c.c.} \quad (81)$$

where the pump magnetic field vector points transversely to the membrane immediately outside of its right surface, with  $\mathcal{B}_p$  being the complex amplitude of the pump magnetic field.

Similarly, let the “seed” idler magnetic field just outside of the right surface of the membrane have the form

$$B_i = \mathcal{B}_i \exp(-i\omega_i t) + \text{c.c.} \quad (82)$$

which is a vector parallel to the magnetic field vector of the pump wave immediately outside of its right surface, with  $\mathcal{B}_i$  being the complex amplitude of the idler magnetic field. We shall assume that the pump is tuned to be on resonance with the upper member of the spectral doublet of the “double” Fabry-Perot (see Figure 3), and that the idler is tuned to be on resonance with the lower member of this doublet. However, the off-resonance, parasitic “anti-Stokes” (i.e., the Doppler up-shifted) frequency component arising from the motion of the membrane will be suppressed, and hence neglected.

To calculate the coefficient of parametric amplification, let us assume that the pump wave is much stronger than both a very weak “seed” idler wave and a very weak “seed” signal wave, so that  $|\mathcal{B}_p| \gg |\mathcal{B}_i|$  and  $|\mathcal{B}_p| \gg |\mathcal{B}_s|$ . It follows from (78) and (82) that the square of the total magnetic field evaluated at the right surface of the “membrane” will have the form

$$B^2 = (B_p + B_i)^2 = (\mathcal{B}_p \exp(-i\omega_p t) + \mathcal{B}_i \exp(-i\omega_i t) + \text{c.c.})^2 \quad (83)$$

If we define the “beat frequency” as

$$\Omega = \omega_p - \omega_i \quad (84)$$



then we see that there will arise cross terms in the square of the magnetic field (83) which will contain terms that vary at the beat frequency  $\Omega$ , viz.,

$$\begin{aligned} (B^2)_\Omega &= \mathcal{B}_p \exp(-i\omega_p t) \mathcal{B}_i^* \exp(+i\omega_i t) + \text{c.c.} \\ &= \mathcal{B}_p \mathcal{B}_i^* \exp(-i\Omega t) + \text{c.c.} \end{aligned} \quad (85)$$

Therefore there will exist a pressure being exerted on the membrane that varies at the beat frequency  $\Omega$  of the form

$$(P)_\Omega = \frac{1}{2\mu_0} (B^2)_\Omega = \frac{1}{2\mu_0} (\mathcal{B}_p \mathcal{B}_i^* \exp(-i\Omega t) + \text{c.c.}) \quad (86)$$

If we define the complex pressure amplitude  $\mathcal{P}_\Omega$  as follows:

$$\mathcal{P}_\Omega = \frac{1}{2\mu_0} \mathcal{B}_p \mathcal{B}_i^* \quad (87)$$

then the pressure exerted on the membrane which varies at the beat frequency  $\Omega$  will have the form

$$(P)_\Omega = \mathcal{P}_\Omega \exp(-i\Omega t) + \text{c.c.} \quad (88)$$

But the beat frequency  $\Omega$  will be assumed to be tuned into resonance with the signal frequency, i.e.,

$$\Omega = \omega_p - \omega_i = \omega_s \quad (89)$$

so that the membrane can be driven at the resonance frequency  $\omega_s$  of the “single” Fabry-Perot resonator to the left of the membrane. Thus power from the right side of the membrane can be fed resonantly by the motion of the membrane into the signal “seed” waveform on the left side.

Due to the presence of the electrostatic charge  $+q$  on the left surface of the membrane, and the relationship

$$F_z(t) = qE_z(t) \quad (90)$$

where  $F_z(t)$  is the Coulomb force on the membrane exerted on the charge  $+q$  by the longitudinal electric field  $E_z(t)$  of a transverse magnetic mode of the “single” Fabry-Perot resonator on the left side of the membrane [21], it follows that the motion of the membrane in the longitudinal  $z$  direction will be “slaved” through  $E_z(t)$  to the dynamics of this transverse magnetic mode [21, Appendix B, where it was shown that one only needs  $q \approx 20$  pC for the Coulomb force to dominate the dynamics of the membrane]. This is due to the tight coupling between  $\Delta z(t)$  and  $E_z(t)$  which arises from the electrostatic charge  $+q$  [29].

Hence let us introduce an Ansatz that the displacement of the membrane has the form

$$(\Delta z(t))_\Omega = \varepsilon_\Omega(t) \exp(-i\Omega t) + \text{c.c.} \quad (91)$$

where  $\varepsilon_\Omega(t)$  is some *slowly-varying* complex displacement amplitude of the membrane, which is the slowly-varying envelope of the *fast* beat frequency phase factor  $\exp(-i\Omega t)$ .

Hence the velocity of the membrane will have the form

$$(v)_\Omega = \frac{d(\Delta z)_\Omega}{dt} \approx v_\Omega(t) \exp(-i\Omega t) + \text{c.c.} \quad (92)$$

where the *slowly-varying* complex velocity amplitude of the moving membrane is

$$v_\Omega(t) \approx -i\Omega \varepsilon_\Omega(t) \quad (93)$$

within the “slowly varying envelope approximation” [30], and the acceleration of the membrane will have the form

$$(a)_\Omega = \left( \frac{dv}{dt} \right)_\Omega \approx \alpha_\Omega(t) \exp(-i\Omega t) + \text{c.c.} \quad (94)$$

where the *slowly-varying* complex acceleration amplitude of the moving membrane is

$$\alpha_\Omega(t) \approx -\Omega^2 \varepsilon_\Omega(t) \quad (95)$$

also within the slowly varying envelope approximation.

The force due to the pressure (86) being exerted on the membrane will have the form

$$(F)_\Omega = \mathcal{F}_\Omega(t) \exp(-i\Omega t) + \text{c.c.} \quad (96)$$

where the *slowly-varying* complex force amplitude acting on the membrane is

$$\mathcal{F}_\Omega(t) = \frac{1}{\mu_0} \mathcal{B}_p \mathcal{B}_i^*(t) \mathcal{A}_{\text{eff}} \quad (97)$$

where  $\mathcal{A}_{\text{eff}}$  is the effective area of the membrane, and where, in the “undepleted pump” approximation [20], we have assumed that the pump amplitude  $\mathcal{B}_p$  is independent of time, but that the idler amplitude  $\mathcal{B}_i^*(t)$  can be a slowly varying function of time due to its amplification.

Then the time-averaged mechanical power fed into the membrane’s motion from the radiation, and hence into the signal wave of the “single” Fabry-Perot cavity of Figure 4, using (93) and (97), is

$$\begin{aligned} \left\langle \frac{dW}{dt} \right\rangle_{\text{signal}} &= \langle F \cdot v \rangle \\ &= \langle \mathcal{F}_\Omega \cdot v_\Omega^* + \text{c.c.} \rangle = \langle \mathcal{F}_\Omega \cdot i\Omega \varepsilon_\Omega + \text{c.c.} \rangle \\ &= -2\text{Im}(\mathcal{F}_\Omega \Omega \varepsilon_\Omega^*) = -2\text{Im} \left( \frac{1}{\mu_0} \mathcal{B}_p \mathcal{B}_i^*(t) \mathcal{A}_{\text{eff}} \cdot \Omega \varepsilon_\Omega^*(t) \right) \end{aligned} \quad (98)$$

Let the complex amplitudes of the pump, idler, and signal waveforms have the complex polar forms

$$\mathcal{B}_p = |\mathcal{B}_p| \exp(i\phi_p) \quad (99)$$

$$\mathcal{B}_i = |\mathcal{B}_i| \exp(i\phi_i) \quad (100)$$

$$\varepsilon_\Omega = |\varepsilon_\Omega| \exp(i\phi_s) \quad (101)$$

By inspection of (98), we see that the maximum power transfer from the radiation fields into the membrane’s motion occurs when the phases of pump, signal, and idler waveforms (i.e., (99), (100), and (101)) are adjusted so as to satisfy the condition

$$\phi_p - \phi_i - \phi_s = -\frac{\pi}{2} \quad (102)$$

whereupon the maximum mechanical power fed into the membrane becomes

$$\left\langle \frac{dW}{dt} \right\rangle_{\text{max, signal}} = + \frac{2\mathcal{A}_{\text{eff}}\Omega}{\mu_0} |\mathcal{B}_p| |\mathcal{B}_i(t)| |\varepsilon_\Omega(t)| \quad (103)$$

Neglecting for the moment all dissipative losses, the kinetic energy of the membrane must *grow* due to this *positive* mechanical power being fed into it. Hence, invoking the principle of the conservation of energy, we get the equation

$$\left\langle \frac{dW}{dt} \right\rangle_{\text{max, signal}} = \frac{d}{dt} \left( \frac{1}{2} m \langle v^2 \rangle \right) = \frac{d}{dt} \left( m\Omega^2 |\varepsilon_\Omega(t)|^2 \right) \quad (104)$$

where we have used (93) and the fact that  $\langle v^2 \rangle = 2|v_\Omega|^2$ . Therefore

$$\frac{d}{dt} \left( m\Omega^2 |\varepsilon_\Omega|^2 \right) = 2m\Omega^2 |\varepsilon_\Omega| \frac{d|\varepsilon_\Omega|}{dt} = \frac{2\mathcal{A}_{\text{eff}}\Omega}{\mu_0} |\mathcal{B}_p| |\mathcal{B}_i| |\varepsilon_\Omega| \quad (105)$$

We thus arrive at an ODE for the rate of growth of the magnitude  $|\varepsilon_\Omega|$  of the displacement of the membrane

$$\frac{d|\varepsilon_\Omega|}{dt} = \frac{\mathcal{A}_{\text{eff}}}{\mu_0 m \Omega} |\mathcal{B}_p| |\mathcal{B}_i| \quad (106)$$

Next, we shall obtain a similar ODE for the rate of growth of the magnitude  $|\mathcal{B}_i|$  of the idler wave. We start from the motional EMF created by the motion of the vibrating SC membrane, which leads to the generation of the motional electric field

$$\mathbf{E} = \mathbf{v} \times \mathbf{B} \quad (107)$$

This relationship implies that the sinusoidal, back-and-forth motion of the mirror at a frequency  $\Omega$  will be modulating the magnetic field oscillating at the pump frequency  $\omega_p$ , such that an idler electric field at the surface of the mirror oscillating at the idler frequency  $\omega_i$  will be generated, i.e.,

$$(\mathbf{E})_i = (\mathbf{v})_\Omega \times (\mathbf{B})_p \quad (108)$$

This is a manifestation of the Doppler effect, in which the sinusoidal motion of the mirror will produce Stokes and anti-Stokes sidebands around the pump frequency  $\omega_p$ . However, due to the doublet spectrum depicted in Figure 3 in the “double” Fabry-Perot resonator, only the down-shifted, first-order Stokes sideband will be resonant with the resonator. Therefore we shall neglect henceforth the anti-Stokes sideband, and all the other higher order Doppler sidebands.

Note that when the membrane is moving towards the left in Figure 4, which is the direction in which the magnetic pressure due to the pump wave is pushing, this pressure will deliver power into the motion of the moving membrane, and *simultaneously*, will deliver power into the red-shifted, first-order Doppler sideband, i.e., the idler wave, via the relationship (108). This will lead to parametric amplification of the membrane’s motion.

Using the Cartesian coordinate system shown in Figure 4, we shall assume that the instantaneous velocity of the mirror is pointing in the  $-z$  direction, and that the instantaneous pump magnetic field vector  $\mathbf{B}_p$  is pointing in  $+x$  direction, so that the instantaneous motional  $\mathbf{E}$  field will be pointing in the  $+y$  direction. Thus, in terms of the complex amplitudes, (108) reduces down to

$$\mathcal{E}_i = v_\Omega^* \mathcal{B}_p \quad (109)$$

Now the time-averaged power delivered into the idler wave by the motional  $\mathbf{E}$  field acting on the current density  $\mathbf{j}$  induced by the idler wave at the right surface of the SC mirror, is

$$\left\langle \frac{dW}{dt} \right\rangle_{\text{idler}} = \int \langle \mathbf{j} \cdot \mathbf{E} \rangle dV = (j_i^* \mathcal{E}_i) \mathcal{A}_{\text{eff}} \delta + \text{c.c.} \quad (110)$$

where  $j_i^*$  is the complex conjugate of the supercurrent density amplitude flowing on the surface of the mirror at the idler frequency  $\omega_i$ ,  $\mathcal{E}_i$  is the complex motional electric field amplitude at  $\omega_i$ ,  $\mathcal{A}_{\text{eff}}$  is the effective focal area of the membrane, and  $\delta$  is the London penetration depth, within which the supercurrents  $j_i^*$  will be flowing near the surface of the membrane. To calculate  $j_i^*$  in (110), we use Ampere’s circuital law and a rectangular loop straddling the surface of the SC mirror, to get

$$\mathcal{B}_i^* = \mu_0 j_i^* \delta \quad (111)$$

where  $\delta$  is London’s penetration depth. Solving for  $j_i^*$  from (111), and substituting it into (110) using (109), we get

$$\begin{aligned} \left\langle \frac{dW}{dt} \right\rangle_{\text{idler}} &= \frac{1}{\mu_0} (v_\Omega^* \mathcal{B}_p \mathcal{B}_i^*) \mathcal{A}_{\text{eff}} + \text{c.c.} \\ &= \frac{1}{\mu_0} ((i\Omega \mathcal{E}_\Omega^*) \mathcal{B}_p \mathcal{B}_i^*) \mathcal{A}_{\text{eff}} + \text{c.c.} \end{aligned} \quad (112)$$

where in the last step we used (93) for the complex conjugate of the complex velocity amplitude  $v_\Omega^*$  of the membrane.

To maximize the power transferred to the idler, we again choose the phase condition (102) between the pump, idler and signal complex amplitudes, and find

$$\left\langle \frac{dW}{dt} \right\rangle_{\text{max, idler}} = + \frac{2}{\mu_0} \Omega |\mathcal{E}_\Omega| |\mathcal{B}_p| |\mathcal{B}_i| \mathcal{A}_{\text{eff}} \quad (113)$$

Assuming the absence of all dissipation, and invoking once again the principle of the conservation of energy, but this time for the idler wave, we obtain

$$\begin{aligned} \left\langle \frac{dW}{dt} \right\rangle_{\text{max, idler}} &= \frac{d}{dt} \left( \frac{1}{2\mu_0} \langle B_i^2 \rangle \right) \mathcal{A}_{\text{eff}} \mathcal{L}_{\text{eff}} = \frac{d}{dt} \left( \frac{1}{\mu_0} |\mathcal{B}_i|^2 \right) \mathcal{A}_{\text{eff}} \mathcal{L}_{\text{eff}} \\ &= +\frac{2}{\mu_0} \Omega |\varepsilon_\Omega| |\mathcal{B}_p| |\mathcal{B}_i| \mathcal{A}_{\text{eff}} \end{aligned} \quad (114)$$

where  $\mathcal{L}_{\text{eff}}$  is the effective length of the “double” Fabry-Perot resonator. We thus arrive at an ODE for the rate of growth of the idler wave

$$\frac{d}{dt} |\mathcal{B}_i| = \frac{\Omega}{\mathcal{L}_{\text{eff}}} |\varepsilon_\Omega| |\mathcal{B}_p| = K_2 |\varepsilon_\Omega| \quad (115)$$

where the constant of proportionality  $K_2$  is

$$K_2 = \frac{\Omega}{\mathcal{L}_{\text{eff}}} |\mathcal{B}_p| \quad (116)$$

Note that this is of the same form as the ODE for the rate of growth of the signal wave [29] obtained earlier in (106), viz.,

$$\frac{d}{dt} |\varepsilon_\Omega| = \frac{\mathcal{A}_{\text{eff}}}{\mu_0 m \Omega} |\mathcal{B}_p| |\mathcal{B}_i| = K_1 |\mathcal{B}_i| \quad (117)$$

where the constant of proportionality  $K_1$  is

$$K_1 = \frac{\mathcal{A}_{\text{eff}}}{\mu_0 m \Omega} |\mathcal{B}_p| \quad (118)$$

This implies that there exists a mutual enhancement of the signal and idler waves that leads to their *exponential* growth, i.e., to the *parametric amplification* of both waves. To see this, let us rewrite the two equations (115) and (117) in the following  $2 \times 2$  matrix form:

$$\frac{d}{dt} \begin{pmatrix} |\varepsilon_\Omega| \\ |\mathcal{B}_i| \end{pmatrix} = \begin{pmatrix} 0 & K_1 \\ K_2 & 0 \end{pmatrix} \begin{pmatrix} |\varepsilon_\Omega| \\ |\mathcal{B}_i| \end{pmatrix} = \Lambda \begin{pmatrix} |\varepsilon_\Omega| \\ |\mathcal{B}_i| \end{pmatrix} \quad (119)$$

where  $\Lambda$  is the eigenvalue of the  $2 \times 2$  matrix, viz.,

$$\Lambda = \pm \sqrt{K_1 K_2} = \pm \sqrt{\frac{\mathcal{A}_{\text{eff}} |\mathcal{B}_p|^2}{\mu_0 m \mathcal{L}_{\text{eff}}}} \quad (120)$$

The solution of (119) is

$$\begin{pmatrix} |\varepsilon_\Omega| \\ |\mathcal{B}_i| \end{pmatrix} = \begin{pmatrix} |\varepsilon_\Omega| \\ |\mathcal{B}_i| \end{pmatrix}_{t=0} \exp(\Lambda t) \quad (121)$$

The meaning of the *positive* root for  $\Lambda$  is that it represents the rate of exponential *growth* of the amplitudes of the coupled signal and idler waves, when the phase condition (102),  $\phi_p - \phi_i - \phi_s = -\pi/2$ , for maximum power *delivery* to these coupled waves, is satisfied, whereas the *negative* root for  $\Lambda$  is that it represents the rate of exponential *decay* of the amplitudes of the coupled signal and idler waves, when the anti-phase condition,  $\phi_p - \phi_i - \phi_s = +\pi/2$ , for maximum power *extraction* from these coupled waves, is satisfied. Whether one gets exponential growth or exponential decay of the waves thus depends on the choices of the initial phases of the pump, signal, and idler waves. This kind of *phase-dependent* amplification is the signature of the production of a *squeezed state* of the vacuum.

Next, let us introduce a dissipative loss phenomenologically into the ODE for the idler (115) as follows:

$$\frac{d}{dt} |\mathcal{B}_i| - \frac{2}{\tau_i} |\mathcal{B}_i| = K_2 |\varepsilon_\Omega| \quad (122)$$

where  $\tau_i$  is the ‘‘cavity ring-down time’’ for the energy stored in the idler cavity mode on the right side of the membrane after the pump wave has been suddenly shut off, and, similarly, into the ODE for the signal (117) as follows:

$$\frac{d}{dt} |\epsilon_\Omega| - \frac{2}{\tau_s} |\epsilon_\Omega| = K_1 |\mathcal{B}_i| \quad (123)$$

where  $\tau_s$  is the ‘‘cavity ring-down time’’ for the energy stored in the signal cavity mode on the left side of the membrane after the pump wave has been suddenly shut off. The relationships between the cavity ring-down times  $\tau_i$  and  $\tau_s$  of the two cavity modes, and their loaded quality factors  $Q_i$  and  $Q_s$ , are

$$Q_i = \omega_i \tau_i \quad (124)$$

$$Q_s = \omega_s \tau_s \quad (125)$$

At the threshold of parametric oscillation, there is a balance between gain and loss such that there arises a steady-state situation in which

$$\frac{d}{dt} |\mathcal{B}_i| = \frac{d}{dt} |\epsilon_\Omega| = 0 \quad (126)$$

Therefore, at threshold, the two ODE’s (122) and (123) reduce down to the two algebraic equations

$$-\frac{2}{\tau_i} |\mathcal{B}_i| = K_2 |\epsilon_\Omega| \quad (127)$$

$$-\frac{2}{\tau_s} |\epsilon_\Omega| = K_1 |\mathcal{B}_i| \quad (128)$$

Multiplying the left sides and the right sides of these two equations together, we get

$$\frac{4}{\tau_i \tau_s} = K_2 K_1 \quad (129)$$

By using the relationships (116), (118), (124), and (125), we get from (129) the threshold condition

$$\frac{4\omega_i \omega_s}{Q_i Q_s} = \frac{\mathcal{A}_{\text{eff}} |\mathcal{B}_p|^2}{\mu_0 m \mathcal{L}_{\text{eff}}} = \frac{|\mathcal{B}_p|^2 V_{\text{eff}}}{\mu_0 m \mathcal{L}_{\text{eff}}^2} \quad (130)$$

Since the time-averaged stored energy stored in the pump cavity mode is

$$\langle U_p \rangle = \frac{1}{2\mu_0} \langle B_p^2 \rangle V_{\text{eff}} = \frac{1}{\mu_0} |\mathcal{B}_p|^2 V_{\text{eff}} \quad (131)$$

we arrive from (130) at the conclusion that the threshold condition is

$$\langle U_p \rangle_{\text{threshold}} = \frac{4m\omega_i \omega_s \mathcal{L}_{\text{eff}}^2}{Q_i Q_s} \quad (132)$$

This is to be compared with Braginski’s threshold condition (72) [27]

$$\langle U_p \rangle_{\text{threshold}}^{\text{Braginski}} = \frac{1}{2} \frac{m\omega_s^2 L^2}{Q_i Q_s} \quad (133)$$

The above two expressions agree as to an order-of-magnitude estimate for the threshold of parametric oscillation for the ‘‘triple’’ Fabry-Perot resonator configuration of Figure 4.

The required threshold input pump power  $\langle P_p \rangle_{\text{threshold}}$  for parametric oscillation due to pump microwaves entering in through the right hole of the ‘‘triple’’ cavity configuration of Figure 4, can be found via the steady-state condition

$$\langle P_p \rangle_{\text{threshold}} = \frac{1}{\tau_p} \langle U_p \rangle_{\text{threshold}} \quad (134)$$

where the quality factor for the pump cavity mode  $Q_p$  is related to the pump cavity ring-down time  $\tau_p$  by

$$Q_p = \omega_p \tau_p \quad (135)$$

Finally, putting this together with (132), we conclude that for parametric oscillation to occur in the configuration of Figure 4, we need to inject a microwave pump power into the “triple” Fabry-Perot cavity the minimum amount of

$$\langle P_p \rangle_{\text{threshold}} = \frac{4m\omega_p\omega_i\omega_s\mathcal{L}_{\text{eff}}^2}{Q_p Q_i Q_s} \quad (136)$$

Numerically, if we assume that [31]

$$m = 2 \text{ mg} \quad (137)$$

$$\omega_p = 2\pi \times 20 \text{ GHz} \quad (138)$$

$$\omega_i \approx \omega_s \approx 2\pi \times 10 \text{ GHz} \quad (139)$$

$$\mathcal{L}_{\text{eff}} \approx \lambda_i/2 \approx \lambda_s/2 \approx 3 \text{ cm} \quad (140)$$

$$Q_p \approx Q_i \approx Q_s \approx 10^{10} \quad (141)$$

then we conclude that we would require a microwave pump power at a frequency of 20 GHz to be injected through the right hole of the “triple” Fabry-Perot cavity of at least

$$\langle P_p \rangle_{\text{threshold}} \approx 4 \text{ microwatts} \quad (142)$$

Above this minimum power level, there would result a parametric oscillation effect in which a macroscopic amount of signal and idler microwaves centered around 10 GHz, with powers on the order of microwatts (i.e., with powers comparable to the pump threshold power), would be emitted in opposite directions through the left and the right holes, respectively, of the “triple” Fabry-Perot cavity, like in a laser. If the  $Q$  is lowered by opening the outcoupling holes, the threshold will go up, but so will the output power of the parametric oscillator. For example, by lowering all the  $Q$ 's to  $10^9$  instead of  $10^{10}$ , the threshold will be increased to 400 microwatts, but the output power of the dynamical Casimir effect will also increase by a few milliwatts. It should be stressed that the leftmost cavity, that is, the “single” Fabry-Perot resonator of Figure 4, is initially devoid of any radiation (i.e., it is initially an *empty* cavity), so that the emission of a macroscopic amount of signal microwaves through the left hole from the left side of the apparatus, would be a dramatic manifestation of the dynamical Casimir effect, in which the observed signal output must have built up exponentially starting solely from vacuum fluctuations inside this initially empty resonator. Since the dynamical Casimir effect is closely related to Hawking radiation according to [32], an observation of parametric oscillation resulting from the moving SC membrane in Figure 4 would be a very interesting result from the point of view of quantum field theory.

## 4 The gravitational dynamical Casimir effect, and the generation of coherent gravitational radiation

In this final section, we speculate that the above ideas can be extended to include the case of gravitational radiation. The physical concept that ties all these ideas together is the crucial use of the DeWitt minimal coupling rule in all of them.

In particular, we briefly comment on the possibility of extending the “separated parametric oscillator” idea for generating EM microwaves by means of the vibrating SC membrane placed inside the extremely high  $Q$  “triple” SC cavity, as depicted in Figure 4, to the much more speculative idea of generating GR microwaves using the same vibrating SC membrane inside the same “triple” SC cavity. This extension is based on the fact that the interaction Hamiltonian  $H_{\text{h,h}}$  in (39) is mathematically identical to that of the interaction Hamiltonian  $H_{\text{A,A}}$  in (38). Furthermore, we are assuming that it is permissible for gravitational radiation fields to be second quantized (see (42)).

However, for this extension of the parametric oscillator idea to work, it is crucial that the walls SC cavity, including the surfaces of the moving SC membrane, reflect GR microwaves with as high a reflectivity as in the case of EM microwaves. In the paper “Do mirrors for gravitational waves exist?” [33], it was predicted that even *thin* SC films are highly reflective mirrors for GR plane waves. This surprising prediction was based on the DeWitt minimal coupling rule (20) applied to the Ginzburg-Landau theory of superconductivity. The “off-diagonal long-range order” (ODLRO) [34] nature of the Cooper pairs causes these pairs to behave *differently* from the ions in the ionic lattice, for which ODLRO does not exist. As a result, inside the SC thin film, the Cooper pairs, which exhibit constructive AB interference, *do not* undergo geodesic motion, in contrast to the ions, which *do* undergo geodesic motion, in response to incident GR radiation. This *difference* in the internal motions of the Cooper pairs and of the ions inside the SC in the presence of GR radiation, leads to a charge separation effect induced by an incoming GR plane wave, such that a huge back-action of the SC film on the GR wave that causes its reflection, results.

If such SC mirrors for GR waves were indeed to exist in Nature, then moving SC mirrors would not only be able to do work like a piston on these waves, but would also simultaneously lead to a Doppler effect that leads to the exponential amplification of these waves above the threshold for parametric oscillation, as explained above. Thus, a laser-like generation of coherent GR waves starting from vacuum fluctuations should become possible. If so, a Hertz-like experiment for GR radiation at microwave frequencies [15] would become feasible to perform.

## 5 Acknowledgements

DAS acknowledges the support of a 2012-2013 Fulbright Senior Scholar Grant.

## References

- [1] M.A. Hohensee, B. Estey, P. Hamilton, A. Zeilinger, and H. Müller, “Force-free gravitational redshift: Proposed gravitational Aharonov-Bohm experiment,” *Phys. Rev. Lett.* **108**, 230404 (2012). Here we consider a thought experiment to see the *vector* gravitational AB effect instead of the *scalar* gravitational AB effect.
- [2] Y. Aharonov and G. Carmi, “Quantum aspects of the equivalence principle,” *Foundations of Physics* **3**, 493 (1973).
- [3] E.G. Harris, “The gravitational Aharonov-Bohm effect with photons,” *Am. J. Phys.* **64**, 378 (1996). Here we consider the AB effect with electrons rather than photons. The AB effect with photons could be understood entirely classically in terms of classical EM waves diffracting around a “solenoid.” However, no such classical explanation would exist for the electron interference experiment described in Figure 1. See also J.M. Cohen and B. Mashhoon, “Standard clocks, interferometry, and gravitomagnetism,” *Phys. Lett. A* **181**, 353 (1993), and A. Tartaglia, “Gravitational Aharonov-Bohm effect and gravitational lensing” gr-qc/00033030.
- [4] V.B. Braginsky, C.M. Caves, and K.S. Thorne, “Laboratory experiments to test relativistic gravity,” *Phys. Rev. D* **15**, 2047 (1977). See also R.L. Forward, “General relativity for the experimentalist,” *Proc. IRE* **49**, 892 (1961), A. Tartaglia and M.L. Ruggiero, “Gravito-electromagnetism versus electromagnetism,” *Eur. J. Phys.* **25**, 203 (2004), section 4.4 of [7], and M. Agop, C.Gh. Buzea, and P. Nica, “Local gravitoelectromagnetic effects on a superconductor,” *Physica C* **339**, 130 (2000).
- [5] The constant  $\epsilon_g$  is determined by the Newtonian limit of (1), which must yield Newton’s law of gravitation, with Newton’s constant  $G$  determined by Cavendish’s experiment.
- [6] The constant  $\mu_g$  is fixed by the fact that when it is combined with the constant  $\epsilon_g$  to form the expression  $1/\sqrt{\epsilon_g\mu_g}$ , one obtains the vacuum speed of light  $c$ .
- [7] R.M. Wald, *General Relativity* (University of Chicago Press, Chicago, 1984).

- [8] H. Weyl, *The Theory of Groups and Quantum Mechanics* (Dover, 1950). The meaning of the arrow in “ $a \rightarrow b$ ” is that “ $a$  is to be replaced by  $b$  in all the following equations.”
- [9] In B.S. DeWitt’s paper, “Superconductors and gravitational drag,” *Phys. Rev. Lett.* **16**, 1092 (1966), the minimal coupling rule (20) was derived starting from Einstein’s field equations. See also G. Papini, “A test of general relativity by means of superconductors,” *Phys. Lett.* **23**, 418 (1966), and “Detection of inertial effects using superconducting interferometers,” *Phys. Lett.* **24A**, 32 (1967).
- [10] We follow the notation and sign conventions of MTW [35], i.e., Greek indices denote spacetime indices running from 0 to 3; Latin indices denote spatial indices running from 1 to 3; repeated indices are summed; the signature of the Minkowski metric is  $\text{diag}(-1, +1, +1, +1)$ .
- [11] L.D. Landau and E.M. Lifshitz, *The Classical Theory of Fields*, 4th Edition: Volume 2 (Butterworth-Heinemann, 2000).
- [12] M.V. Berry, “Quantal phase factors accompanying adiabatic changes,” *Proc. R. Soc. Lond. A* **392**, 45 (1984).
- [13] S.B. Felch, J. Tate, B. Cabrera, and J.T. Anderson, “Precise determination of  $h/m_e$  using a rotating, superconducting ring,” *Phys. Rev. B* **31**, 7006 (1985). There remain some small, unexplained discrepancies for the inferred electron mass, which are probably due to some unknown systematic errors in the experiment. See also M.D. Semon, “Experimental verification of an Aharonov-Bohm effect in rotating reference frames,” *Foundations of Physics* **7**, 49 (1982).
- [14] It should be noted that the use of the time-dependent gauge in which  $(\mathbf{h}(\mathbf{r}, t))_i = ch_{0i}(\mathbf{r}, t) \neq 0$  in this context is only considered for fields within matter, and not in vacuum, where the time-dependent transverse-traceless gauge would be more appropriate.
- [15] R.Y. Chiao, “New directions for gravitational-wave physics via ‘Millikan oil drops’,” in *Visions of Discovery*, edited by R.Y. Chiao, M.L. Cohen, A.J. Leggett, W.D. Phillips, and C.L. Harper, Jr. (Cambridge University Press, 2011), p. 348.
- [16] J.C. Garrison and R.Y. Chiao, *Quantum Optics* (Oxford, 2008), Equation (2.103).
- [17] J.C. Garrison and R.Y. Chiao, *Quantum Optics* (Oxford, 2008), Equation (15.30).
- [18] M. Aspelmeyer, P. Meystre, and K. Schwab, “Quantum optomechanics,” *Phys. Today* **65**, 29 (2012).
- [19] S. Kuhr, S. Gleyzes, C. Guerlin, J. Bernu, U.B. Hoff, S. Deléglise, S. Osnaghi, M. Brune, J.M. Raimond, S. Haroche, E. Jacques, P. Bosland, and B. Visentin, “Ultrahigh finesse Fabry-Perot superconducting resonator,” *Appl. Phys. Lett.* **90**, 164101 (2007).
- [20] R.W. Boyd, *Nonlinear Optics* (Academic Press 2003).
- [21] R.Y. Chiao, L.A. Martinez, S.J. Minter, A. Trubarov, “Parametric oscillation of a moving mirror driven by radiation pressure in a superconducting Fabry-Perot resonator system,” *Phys. Scr. T* **151**, 014073 (2012); arXiv: 1207.6885.
- [22] M. Philipp, P. von Brentano, G. Pascovici, and A. Richter, “Frequency and width crossing of two interacting resonances in a microwave cavity,” *Phys. Rev. E* **62**, 1922 (2000).
- [23] I.G. Wilson, C.W. Schramm, and J.P. Kinzer. “High Q resonant cavities for microwave testing,” *Bell Syst. Tech. J* **25.3** (1946): 408-434.
- [24] D.J. Griffiths, *Introduction to Electrodynamics*, 3rd edition (Prentice Hall, 1999), p. 351.
- [25] J.D. Jackson, *Classical Electrodynamics*, third edition (John Wiley & Sons), p. 261.
- [26] Note that the application of a *magnetic field* to any system of particles with a given charge-to-mass ratio is equivalent, by Larmor’s theorem, to *rotating* the system at the Larmor angular frequency. Thus there exists a natural connection between the  $\mathbf{A}$  and  $\mathbf{h}$  fields in the proposed experiments in Figures 2 and 4.
- [27] V.B. Braginsky, S.E. Strigin, and S.P. Vyatchanin, “Parametric oscillatory instability in Fabry-Perot interferometer,” *Phys. Lett. A* **287**, 331, (2001).



- [28] R.Y. Chiao, “Analysis and estimation of the threshold for a microwave ‘pellicle mirror’ parametric oscillator, via energy conservation,” arXiv:1211.3519.
- [29] If the electrostatic charge  $+q$  on the right side of the membrane were to be sufficiently large (i.e., greater than around 20 picocoulombs; see Appendix B of [21]), so that the membrane becomes extremely tightly coupled to the “single” Fabry-Perot cavity mode on the left side of the membrane, which would happen if this cavity were to be excited in an appropriate transverse magnetic mode, then the mechanical dynamics of the membrane would be “slaved” to the electromagnetic dynamics of this “signal” frequency cavity. For then the displacement of the membrane would be completely determined by Newton’s equation of motion (55), so that there results a fixed relationship between the *instantaneous* longitudinal electric field and the *instantaneous* membrane displacement, which is given by

$$(\epsilon_{\Omega})_s = -\frac{q(\mathcal{E}_z)_s}{m\omega_s^2} \quad (143)$$

where  $(\mathcal{E}_z)_s$  is the complex amplitude of the longitudinal electric field of the transverse magnetic mode at the “signal” frequency  $\omega_s$  of the “single” Fabry-Perot cavity and  $(\epsilon_{\Omega})_s$  is the complex amplitude of the displacement of the membrane, which oscillates at the same frequency  $\omega_s$ . In this way, the mechanical vibration frequency  $\Omega$  of the membrane would be forced to become identical to the microwave frequency  $\omega_s$  of this cavity, and the kinetic energy of the mechanical vibrational motion would be forced to become identical to the electromagnetic energy stored inside this cavity, because these two degrees of freedom would be so tightly coupled to each other that they would no longer be independent degrees of freedom.

- [30] J.C. Garrison and R.Y. Chiao, *Quantum Optics* (Oxford, 2008), p. 89.
- [31] Instead of a solid SC membrane, one could use a grid of fine SC wires, for example, four fine SC wires arranged in a pattern similar to the number sign “#”, in order to reduce the mass, and thus the threshold.
- [32] P.D. Nation, J.R. Johansson, M.P. Blencowe, and F. Nori, “Colloquium: Stimulating uncertainty: Amplifying the quantum vacuum with superconducting circuits,” *Rev. Mod. Phys.* **84**, 1 (2012).
- [33] S.J. Minter, K. Wegter-McNelly, and R.Y. Chiao, “Do mirrors for gravitational waves exist?”, *Physica E* **42**, 234 (2010); arXiv:0903.0661.
- [34] C.N. Yang, “Concept of off-diagonal long-range order and the quantum phases of liquid He and of superconductors,” *Rev. Mod. Phys.* **34**, 694 (1962).
- [35] C.W. Misner, K.S. Thorne, and J.A. Wheeler, *Gravitation* (San Francisco: Freeman, 1972).